Supplementary Information (SI) for ChemComm.
This journal is © The Royal Society of Chemistry 2025

Supplementary Information

Scalable fabrication of nano-to-micro carbon disk ultramicroelectrodes for single small extracellular vesicle detection

Hong-Yuan Liu, An-Rong Sun, Li-Yuan Wu, and Zhi-Ling Zhang*

College of Chemistry and Molecular Sciences, Wuhan University, Wuhan, 430072, People's Republic of China.

** Corresponding author: Zhi-Ling Zhang*

E-mail: zlzhang@whu.edu.cn

Table of content

Experimental Section

S1. Reagents and instruments

S2. Fabrication of scalable UME

S3. Isolation and characterization of small extracellular vesicles from cell culture media

S4. Theoretical calculation of total current(i_{ss}), step signal(Δi) and current density(j) on UME.

Results and Discussion

S5. Illustration of UME fabrication (Fig. S1)

S6. Characterization of UME (Fig. S2)

S7. Characterization of sEVs (Fig. S3)

S8. Theoretical analyses of the signal-to-background ratios variation with UME size (Fig. S5)

S9. Experient collision result of different UME sizes (Fig. S6)

S10. Etching and polish degree affect final UME size (Table S1)

Reference

Experimental Section

S1. Reagents and instruments

All chemicals used in this study, including potassium chloride, potassium ferrocyanide, ferrocene methanol, acetone, ethanol, sodium chloride, sodium dihydrogen phosphate, and disodium hydrogen phosphate dodecahydrate, were of analytical grade and purchased from Sinopharm Chemical Reagent Co., Ltd. (Shanghai, China). Unless otherwise specified, these reagents were used as received without further purification. Milli-Q water, with a resistivity of 18.2 $M\Omega \cdot cm^{-1}$ (Milli-Q Advantage A10), was used throughout the experiments to prepare all aqueous solutions, ensuring the highest purity and preventing contamination.

All the electrochemical measurements were carried out on a CHI-750E electrochemical workstation (CH instruments Inc.) and a CHI Faraday cage (CH instruments Inc.). The electrochemical setup included an Ag/AgCl reference electrode and a platinum (Pt) wire as the counter electrode. The carbon disk UME served as the working electrode, and all measurements were performed at the temperature of 25 ± 1°C.

S2. Fabrication of scalable UME

The carbon disk ultra-microelectrodes (UMEs) were fabricated through a process of etching, insulation, and re-exposure, detailed illustration can be found in Fig. S1. Briefly, a carbon fiber of 7 um in diameter (C005722, Goodfellow Cambridge Limited) was securely attached to a copper wire by conductive epoxy to ensure electrical conductivity. The carbon fiber tip was then ultrasonically cleaned in acetone, ethanol, and water, followed by flame etching. The etching process, performed approximately 25 times (with adjustments made based on the desired final size), involved brief 0.2-second exposures to the flame bottom, resulting in a needle shape with the tip diameter of a size range of several nanometers nm to 7 μm, which maximum equals to the diameter of carbon fiber. After etching, the flame-etched carbon fiber with copper wire was inserted into a capillary (1B100F-4, with an outer diameter of 1.0 mm and an inner diameter of 0.58 mm, World Precision Instruments) that had been pre-heated and shrunk, and carefully. The flame-etched carbon fiber was then insulated by epoxy resin (EPO-TEK 301, Epoxy Technology), followed by curing at 100 °C for 12 hours. Then, the insulated UME was re-exposed by sandpaper and scrub polishing from coarse to fine. The final size of the carbon disk UME could be controlled through variations in the flame etching and polishing processes, yielding dimensions from the nanoscale to the microscale.

S3. Isolation and Characterization of Small Extracellular Vesicles from Cell Culture Media.

The process of sEVs isolation followed Théry's protocol,[1] and the charaerization of sEVs sample followed the guideline published by the International Society for Extracellular Vesicles.[2,3]

HeLa (human cervical carcinoma) cell lines were cultured in Dulbecco's Modified Eagle Medium (DMEM; Gibco) supplemented with 10% (v/v) fetal bovine serum (FBS; PAN Biotech). Cells were maintained in a 5% CO_2 humidified atmosphere at 37 °C in 150 mm Petri dishes (Corning). Once the cells reached 70–80% confluency, the original culture medium containing FBS was removed, and the cells were washed gently with phosphate-buffered saline (PBS) for three times to eliminate residual serum components. Fresh FBS-free DMEM of equivalent volume was then added, and the cells were incubated for 48 hours for sEVs production.

The conditioned medium was harvested and subjected to a series of differential ultracentrifugation steps for sEVs isolation and purification. The medium was sequentially centrifuged at 300 g for 10 minutes, 2000 g for 30 minutes, and 10,000 g for 30 minutes to remove cells, cell debris, and larger vesicles. The small extracellular vesicles were pelleted by ultracentrifugation at 120,000 g for 70 minutes, resuspended with PBS, and subjected to a second ultracentrifugation at 120,000 g for an additional 70 minutes for purification. Centrifugation was done by Multifuge X1R Refrigerated Centrifuge (Thermo Scientific). Ultracentrifugation was done by ultracentrifuge (Optima XE-90, Beckman Coulter), fixed-

angle titanium rotor (Type 70.1 Ti, Beckman Coulter), and centrifuge bottle with cap (355618, Beckman Coulter). All centrifugation steps were performed at 4 °C. The final pellets were resuspended in PBS and stored at −80 °C until further analysis.

Characterization of the isolated sEVs included particle size and zeta potential measurements using nanoparticle tracking analysis (NTA; NS300, NanoSight) and dynamic light scattering (DLS; Zetasizer Ultra, Malvern Panalytical). The morphology and size of the sEVs were further analyzed by transmission electron microscopy (TEM; JEM-2100, JEOL). The protein quantification of sEVs isolated was tested using BCA protein assay kit (C503021, Sangon Biotech).

S4. Theoretical calculation of total current(i_{ss}), step signal(Δi) and current density(j) on UME.

The background or total current of a disk UME can be calculated using the diffusion-limited steady-state current equation: $i_{ss} = 4nFDcr_0$. In this equation: n is the number of electron transfer during oxidation or reduction, F is the Faraday constant, D is the diffusion coefficient, c is the concentration and r_0 is the radius of UME. Since i_{ss} is directly proportional to r_0, a larger UME results in a higher background current.

For theoretical step signal, $\Delta i = f_g 4nFDCr_0(r_p/r_0)^2$ was used for calculation. where f_g is a geometric factor. For average theoretical step signal, f_g was taken as 0.205, simplifying the equation to: $\Delta i = 0.82 \times nFDCr_p^2/r_0$. This expression shows that Δi is inversely proportional to r_0, meaning that a larger UME size may lead to a smaller signal.

The theoretical calculation of steady-state diffusion at a disk UME and corresponding current density distribution are based on Bard's work.[4] The local steady-state current density, j, at any radial position on the electrode surface is given by:

$$j = \frac{2nFD\Delta C(z=0)}{\pi(r_0^2 - r^2)^{1/2}} \qquad \text{Equation S1}$$

In this equation: n is the number of electron transfer during oxidation or reduction, F is the Faraday constant, D is the diffusion coefficient of the redox or oxide species, $\Delta C(z=0)$ is the concentration gradient at the electrode surface (z=0), which can be approximately equal to C_O^*, the the bulk concentration of the redox or oxide species. r_0 represents the radius of the electrode, r denotes the distance from center to point.

Equation S1 describes the spatial variation of current density across the UME surface. Notably, the current density diverges near the electrode edge ($r \to r_0$), reflecting the singularity in the $\sqrt{r_0^2 - r^2}$ term.

To quantify the radial position corresponding to specific percentages of the total current, Equation S1 was integrated numerically. This was implemented in MATLAB using the following approach:

```
% Parameters & definition

n = 1;                      % The number of electron transfer

F = 96485.3321;             % Faraday's constant (C/mol)

D = 6.5e-10;                % Diffusion coefficient of KFCN (m^2/s), can be adjusted upon need

C_bulk = 20;                % Bulk concentration of redox(reactants) (mol/m^3), can be adjusted
                              upon need

R = 3e-7;                   % Radius of UME (m), can be adjusted upon need

num_points = 1000;          % Number of radial points(steps) , can be adjusted upon need

epsilon = 1e-20;            % Small cutoff to avoid singularity

% Radial positions (excluding R to avoid singularity)

r = linspace(0, R, num_points);

r = r(1:end-1);             % Exclude r = R

% Local current density (avoiding singularity), corresponding to Equation S1
```

```
j = (2 * n * F * D * C_bulk) ./ (pi * sqrt(max(R^2 - r.^2, epsilon)));

% Area of differential rings

dr = r(2) - r(1);                % Radial step size

ring_areas = 2 * pi * r * dr;        % Areas of differential rings

% Cumulative current

cumulative_current = cumsum(j .* ring_areas);

% Total current (numerical integration)

I_total = sum(j .* ring_areas);

% Theoretical total current

I_theory = 4 * n * F * D * C_bulk * R;

% Find the radial position for specific percentage of total current

target_current = 0.5 * I_theory;        % target percentage, can be adjusted upon needs

index_50 = find(cumulative_current >= target_current, 1, 'first'); % First index where cumulative current meets/exceeds target

radial_distance_50 = r(index_50);      % Corresponding radial distance

% Output results

fprintf('Theoretical total current (I_theory): %.4e A\n', I_theory);

fprintf('Numerical total current (I_total): %.4e A\n', I_total);
```

```
fprintf('Radial distance for 50%% total current: %.4e m (%.4f μm)\n', radial_distance_50,
radial_distance_50 * 1e6);
```

Results and Discussion

S5. Fabrication of scalable carbon disk UME.

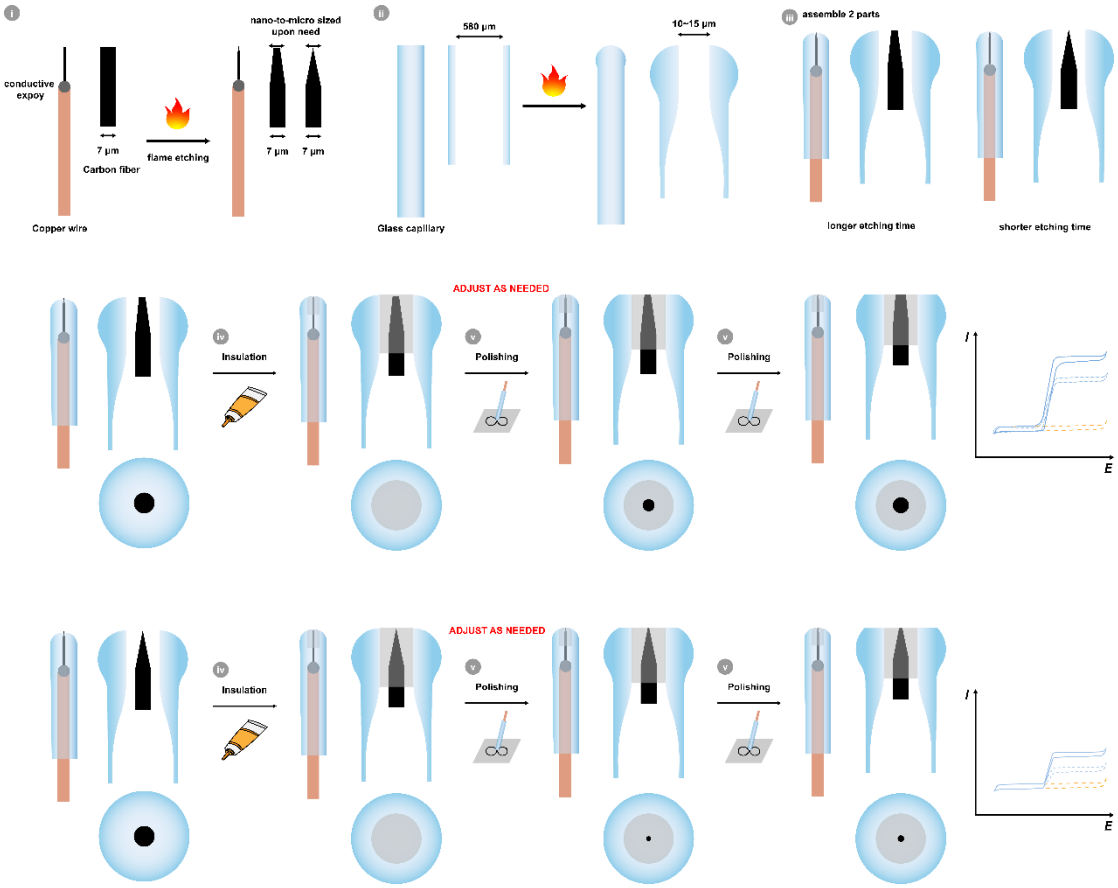

Fig. S1 Detailed illustration of the fabrication process for scalable carbon disk UME.

S6. Characterization of UME

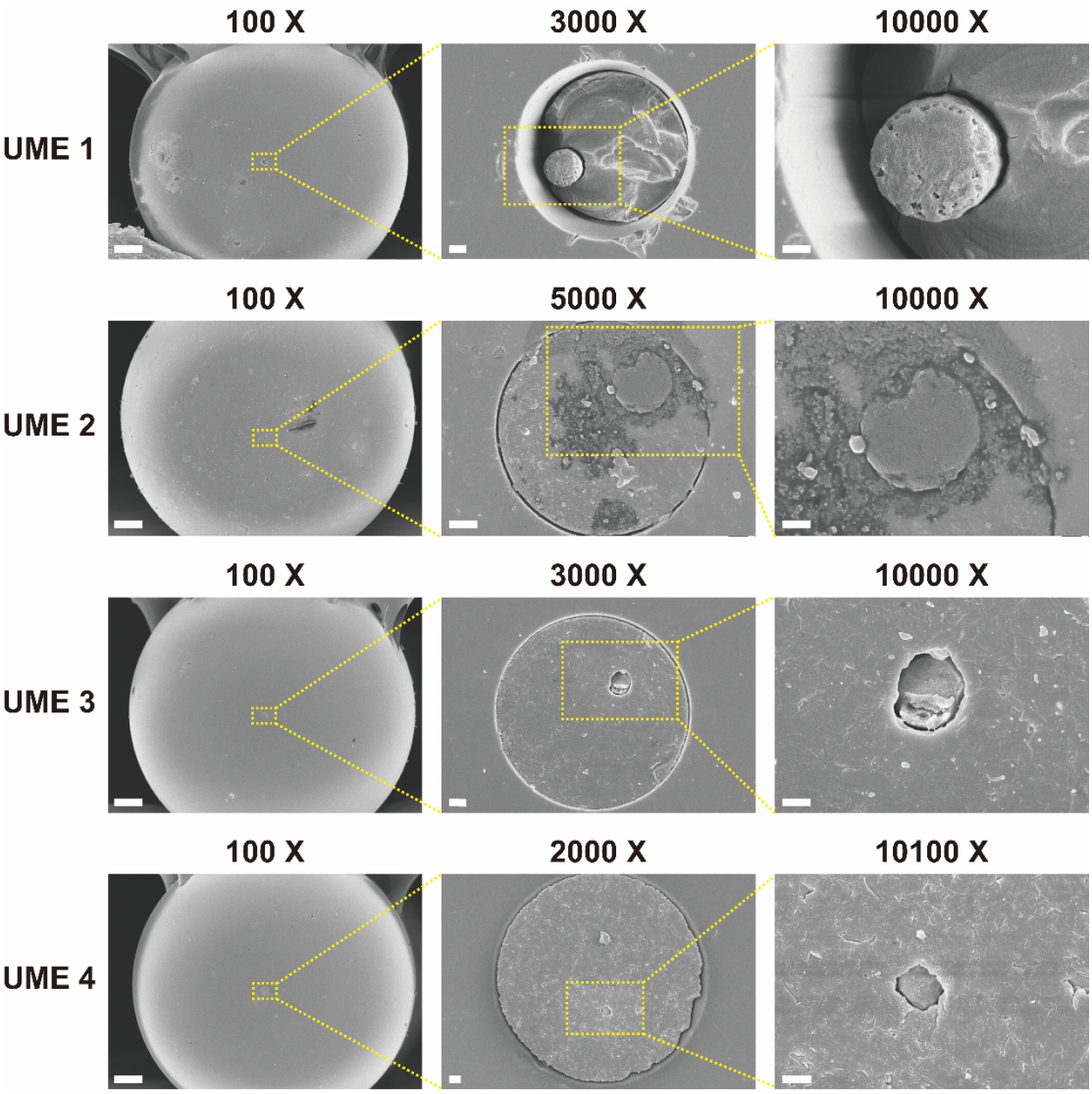

Fig. S2 SEM images of UMEs produced by the fabrication method in this research. The scale bars in the left, center and right row represent 100 μm, 2 μm and 1 μm, respectively.

S7. Characterization of sEVs.

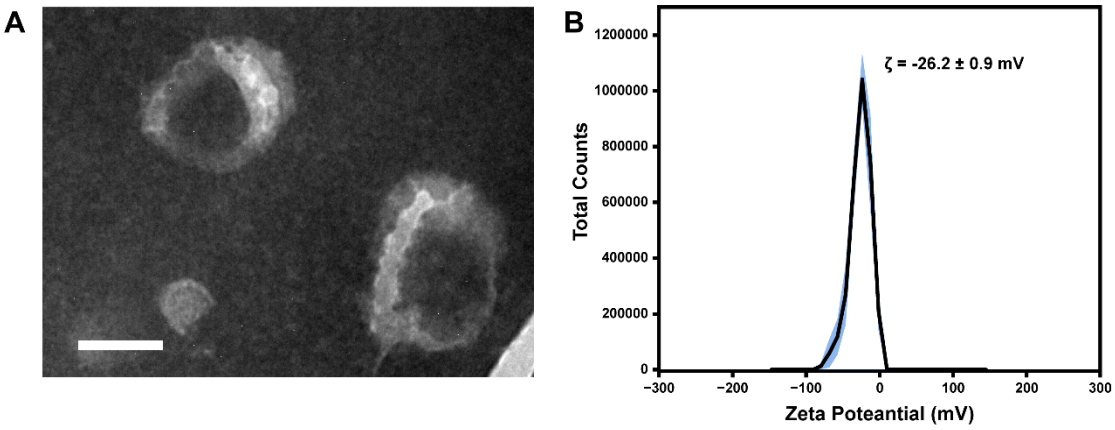

Fig. S3 Characterization of sEVs produced by HeLa cells. (A) TEM images of sEVs. Scale bar: 100 nm. (B) Zeta potential (ZP) of sEVs.

S8. Theoretical analyses of the signal-to-background ratios variation with UME size

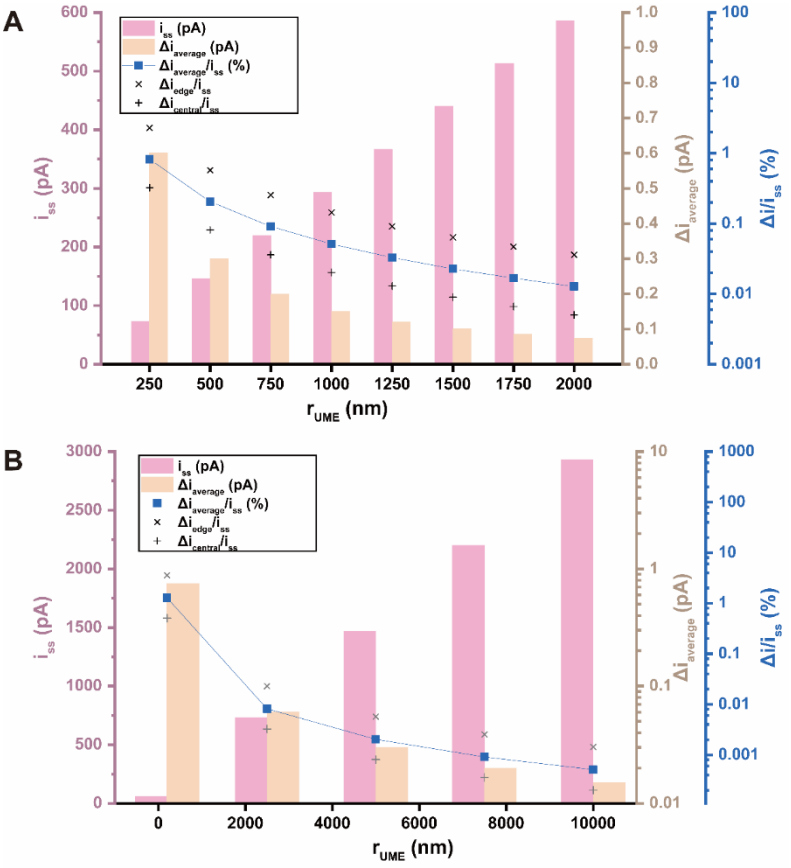

Fig. S4 The influences of UME size on the signal characteristics. (A)&(B) Theoretical values varies with the UME size ($r_{particle}$ = 50 nm). Pink bars (i_{ss}) represent the background diffusion-limited current, while orange bars ($\Delta i_{average}$) represent the average theoretical step signal for each UME size.. Blue squares indicate the average theoretical signal-to-background ratio ($\Delta i_{average}$ / i_{ss}) expressed as a percentage, and grey 'x' and '+' symbols represent the theoretical signal-to-background ratios at edge (Δi_{edge} / i_{ss}) and center (Δi_{center} / i_{ss}) of the UME, respectively.

S9. Experient collision result of different UME sizes

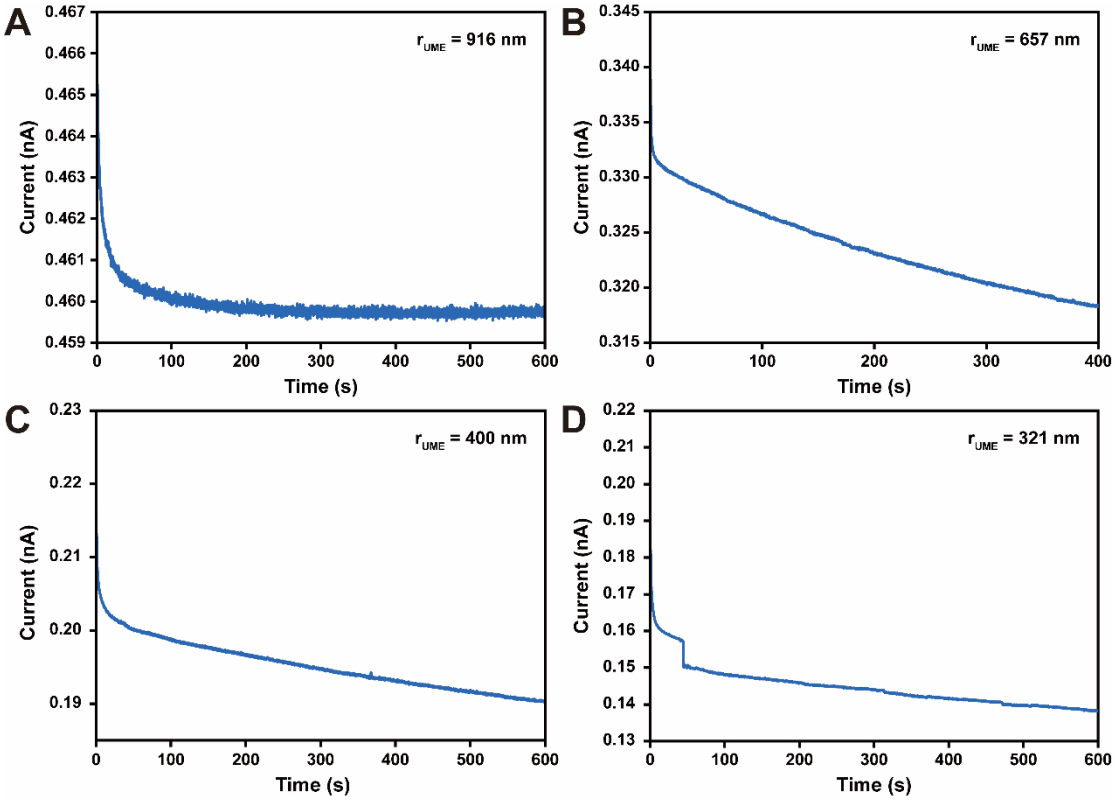

Fig. S5 Blocking collisions with various sizes of UME in 2 mM KFCN.

S10. Etching and polish degree affect final UME size

No	Etching Cycles (0.2s per cycle)	Diameter of Etched carbon fiber	Rough Polish Cycles	Final UME size (diameter)
1	0	~7 μm	20	~ 7 μm
2	20~25	~1 μm	20	~ 1 μm
3	30~40	300 ~500 nm	40	~ 450 nm
4	40~60	50 ~ 200 nm	100	~ 180 nm
5	40~60	50 ~ 200 nm	20	~ 60 nm

Table. S1 Etching and polish degree affect final UME size.

Reference

1 C. Théry, S. Amigorena, G. Raposo and A. Clayton, *Current Protocols in Cell Biology*, 2006, https://doi.org/10.1002/0471143030.cb0322s30.

2 J. A. Welsh, D. C. I. Goberdhan, L. O'Driscoll, E. I. Buzas, C. Blenkiron, B. Bussolati, H. Cai, D. Di Vizio, T. A. P. Driedonks, U. Erdbrügger, J. M. Falcon-Perez, Q.-L. Fu, A. F. Hill, M. Lenassi, S. K. Lim, M. G. Mahoney, S. Mohanty, A. Möller, R. Nieuwland, T. Ochiya, S. Sahoo, A. C. Torrecilhas, L. Zheng, A. Zijlstra, S. Abuelreich, R. Bagabas, P. Bergese, E. M. Bridges, M. Brucale, D. Burger, R. P. Carney, E. Cocucci, R. Crescitelli, E. Hanser, A. L. Harris, N. J. Haughey, A. Hendrix, A. R. Ivanov, T. Jovanovic-Talisman, N. A. Kruh-Garcia, V. Ku'ulei-Lyn Faustino, D. Kyburz, C. Lässer, K. M. Lennon, J. Lötvall, A. L. Maddox, E. S. Martens-Uzunova, R. R. Mizenko, L. A. Newman, A. Ridolfi, E. Rohde, T. Rojalin, A. Rowland, A. Saftics, U. S. Sandau, J. A. Saugstad, F. Shekari, S. Swift, D. Ter-Ovanesyan, J. P. Tosar, Z. Useckaite, F. Valle, Z. Varga, E. van der Pol, M. J. C. van Herwijnen, M. H. M. Wauben, A. M. Wehman, S. Williams, A. Zendrini, A. J. Zimmerman, M. Consortium, C. Théry and K. W. Witwer, *Journal of Extracellular Vesicles*, 2024, **13**, e12404.

3 C. Théry, K. W. Witwer, E. Aikawa, M. J. Alcaraz, J. D. Anderson, R. Andriantsitohaina, A. Antoniou, T. Arab, F. Archer, G. K. Atkin-Smith, D. C. Ayre, J.-M. Bach, D. Bachurski, H. Baharvand, L. Balaj, S. Baldacchino, N. N. Bauer, A. A. Baxter, M. Bebawy, C. Beckham, A. Bedina Zavec, A. Benmoussa, A. C. Berardi, P. Bergese, E. Bielska, C. Blenkiron, S. Bobis-Wozowicz, E. Boilard, W. Boireau, A. Bongiovanni, F. E. Borràs, S. Bosch, C. M. Boulanger, X. Breakefield, A. M. Breglio, M. Á. Brennan, D. R. Brigstock, A. Brisson, M. L. Broekman, J. F. Bromberg, P. Bryl-Górecka, S. Buch, A. H. Buck, D. Burger, S. Busatto, D. Buschmann, B. Bussolati, E. I. Buzás, J. B. Byrd, G. Camussi, D. R. Carter, S. Caruso, L. W. Chamley, Y.-T. Chang, C. Chen, S. Chen, L. Cheng, A. R. Chin, A. Clayton, S. P. Clerici, A. Cocks, E. Cocucci, R. J. Coffey, A. Cordeiro-da-Silva, Y. Couch, F. A. Coumans, B. Coyle, R. Crescitelli, M. F. Criado, C. D'Souza-Schorey, S. Das, A. Datta Chaudhuri, P. de Candia, E. F. De Santana Junior, O. De Wever, H. A. del Portillo, T. Demaret, S. Deville, A. Devitt, B. Dhondt, D. Di Vizio, L. C. Dieterich, V. Dolo, A. P. Dominguez Rubio, M. Dominici, M. R. Dourado, T. A. Driedonks, F. V. Duarte, H. M. Duncan, R. M. Eichenberger, K. Ekström, S. EL Andaloussi, C. Elie-Caille, U. Erdbrügger, J. M. Falcón-Pérez, F. Fatima, J. E. Fish, M. Flores-Bellver, A. Försönits, A. Frelet-Barrand, F. Fricke, G. Fuhrmann, S. Gabrielsson, A. Gámez-Valero, C. Gardiner, K. Gärtner, R. Gaudin, Y. S. Gho, B. Giebel, C. Gilbert, M. Gimona, I. Giusti, D. C. Goberdhan, A. Görgens, S. M. Gorski, D. W. Greening, J. C. Gross, A. Gualerzi, G. N. Gupta, D. Gustafson, A. Handberg, R. A. Haraszti, P. Harrison, H. Hegyesi, A. Hendrix, A. F. Hill, F. H. Hochberg, K. F. Hoffmann, B. Holder, H. Holthofer, B. Hosseinkhani, G. Hu, Y. Huang, V. Huber, S. Hunt, A. G.-E. Ibrahim, T. Ikezu, J. M. Inal, M. Isin, A. Ivanova, H. K. Jackson, S. Jacobsen, S. M. Jay, M. Jayachandran, G. Jenster, L. Jiang, S. M. Johnson, J. C. Jones, A. Jong, T. Jovanovic-Talisman, S. Jung, R. Kalluri, S. Kano, S. Kaur, Y. Kawamura, E. T. Keller, D. Khamari, E. Khomyakova, A. Khvorova, P. Kierulf, K. P. Kim, T. Kislinger, M. Klingeborn, D. J. Klinke II, M. Kornek, M. M. Kosanović, Á. F. Kovács, E.-M. Krämer-Albers, S. Krasemann, M. Krause, I. V. Kurochkin, G. D. Kusuma, S. Kuypers, S. Laitinen, S. M. Langevin, L. R. Languino, J. Lannigan, C. Lässer, L. C. Laurent, G. Lavieu, E. Lázaro-Ibáñez, S. Le Lay, M.-S. Lee, Y. X. F. Lee, D. S.

Lemos, M. Lenassi, A. Leszczynska, I. T. Li, K. Liao, S. F. Libregts, E. Ligeti, R. Lim, S. K. Lim, A. Linē, K. Linnemannstöns, A. Llorente, C. A. Lombard, M. J. Lorenowicz, Á. M. Lörincz, J. Lötvall, J. Lovett, M. C. Lowry, X. Loyer, Q. Lu, B. Lukomska, T. R. Lunavat, S. L. Maas, H. Malhi, A. Marcilla, J. Mariani, J. Mariscal, E. S. Martens-Uzunova, L. Martin-Jaular, M. C. Martinez, V. R. Martins, M. Mathieu, S. Mathivanan, M. Maugeri, L. K. McGinnis, M. J. McVey, D. G. Meckes Jr, K. L. Meehan, I. Mertens, V. R. Minciacchi, A. Möller, M. Møller Jørgensen, A. Morales-Kastresana, J. Morhayim, F. Mullier, M. Muraca, L. Musante, V. Mussack, D. C. Muth, K. H. Myburgh, T. Najrana, M. Nawaz, I. Nazarenko, P. Nejsum, C. Neri, T. Neri, R. Nieuwland, L. Nimrichter, J. P. Nolan, E. N. Nolte-'t Hoen, N. Noren Hooten, L. O'Driscoll, T. O'Grady, A. O'Loghlen, T. Ochiya, M. Olivier, A. Ortiz, L. A. Ortiz, X. Osteikoetxea, O. Østergaard, M. Ostrowski, J. Park, D. M. Pegtel, H. Peinado, F. Perut, M. W. Pfaffl, D. G. Phinney, B. C. Pieters, R. C. Pink, D. S. Pisetsky, E. Pogge von Strandmann, I. Polakovicova, I. K. Poon, B. H. Powell, I. Prada, L. Pulliam, P. Quesenberry, A. Radeghieri, R. L. Raffai, S. Raimondo, J. Rak, M. I. Ramirez, G. Raposo, M. S. Rayyan, N. Regev-Rudzki, F. L. Ricklefs, P. D. Robbins, D. D. Roberts, S. C. Rodrigues, E. Rohde, S. Rome, K. M. Rouschop, A. Rughetti, A. E. Russell, P. Saá, S. Sahoo, E. Salas-Huenuleo, C. Sánchez, J. A. Saugstad, M. J. Saul, R. M. Schiffelers, R. Schneider, T. H. Schøyen, A. Scott, E. Shahaj, S. Sharma, O. Shatnyeva, F. Shekari, G. V. Shelke, A. K. Shetty, K. Shiba, P. R.-M. Siljander, A. M. Silva, A. Skowronek, O. L. Snyder II, R. P. Soares, B. W. Sódar, C. Soekmadji, J. Sotillo, P. D. Stahl, W. Stoorvogel, S. L. Stott, E. F. Strasser, S. Swift, H. Tahara, M. Tewari, K. Timms, S. Tiwari, R. Tixeira, M. Tkach, W. S. Toh, R. Tomasini, A. C. Torrecilhas, J. P. Tosar, V. Toxavidis, L. Urbanelli, P. Vader, B. W. van Balkom, S. G. van der Grein, J. Van Deun, M. J. van Herwijnen, K. Van Keuren-Jensen, G. van Niel, M. E. van Royen, A. J. van Wijnen, M. H. Vasconcelos, I. J. Vechetti Jr, T. D. Veit, L. J. Vella, É. Velot, F. J. Verweij, B. Vestad, J. L. Viñas, T. Visnovitz, K. V. Vukman, J. Wahlgren, D. C. Watson, M. H. Wauben, A. Weaver, J. P. Webber, V. Weber, A. M. Wehman, D. J. Weiss, J. A. Welsh, S. Wendt, A. M. Wheelock, Z. Wiener, L. Witte, J. Wolfram, A. Xagorari, P. Xander, J. Xu, X. Yan, M. Yáñez-Mó, H. Yin, Y. Yuana, V. Zappulli, J. Zarubova, V. Žėkas, J. Zhang, Z. Zhao, L. Zheng, A. R. Zheutlin, A. M. Zickler, P. Zimmermann, A. M. Zivkovic, D. Zocco and E. K. Zuba-Surma, *Journal of Extracellular Vesicles*, 2018, **7**, 1535750.

4 A. J. Bard, L. R. Faulkner and H. S. White, *Electrochemical Methods: Fundamentals and Applications*, John Wiley & Sons, Ltd., Hoboken, NJ, Third edition., 2022.